Life Sciences 219 (2019) 152–162

Contents lists available at ScienceDirect

Life Sciences

journal homepage: www.elsevier.com/locate/lifescie

Phenotypical and functional evaluation of dendritic cells after exosomal delivery of miRNA-155

Ali Asadirad[a], Seyed Mahmoud Hashemi[a,d,*], Kaveh Baghaei[b], Hossein Ghanbarian[c,d,e], Esmaeil Mortaz[a,f], Mohammad Reza Zali[g], Davar Amani[a,**]

[a] Department of Immunology, School of Medicine, Shahid Beheshti University of Medical Sciences, Tehran, Iran
[b] Basic and Molecular Epidemiology of Gastrointestinal Disorder Research Center, Research Institute for Gastroenterology and Liver Disease, Shahid Beheshti University of Medical Science, Tehran, Iran
[c] Cellular and Molecular Biology Research Center, School of Medicine, Shahid Beheshti University of Medical Sciences, Tehran, Iran
[d] Department of Tissue Engineering and Applied Cell Sciences, School of Advanced Technologies in Medicine, Shahid Beheshti University of Medical Sciences, Tehran, Iran
[e] Department of Medical Biotechnology, School of Advanced Technologies in Medicine, Shahid Beheshti University of Medical Sciences, Tehran, Iran
[f] Clinical Tuberculosis and Epidemiology Research Center, National Research Institute of Tuberculosis and Lung Diseases (NRITLD), Shahid Beheshti University of Medical Sciences, Tehran, Iran
[g] Gastroenterology and Liver Diseases Research center, Research institute for Gastroenterology and Liver Diseases, Shahid Beheshti University of Medical Sciences, Tehran, Iran

ARTICLE INFO

Keywords:
Dendritic cells
miRNA-155
Exosome
Electroporation

ABSTRACT

Aims: The clinical efficiency of dendritic cell (DC) therapy needs to be improved. Exosomes, as membrane nanovesicles, carry bio-macromolecules and play essential roles in intercellular crosstalk. Here, it is proposed that tumor cell-derived exosomes could function as vehicles to deliver exogenous miRNA-155 into DCs, for simultaneous miRNA delivery and antigen priming of DCs. Following optimization of the miRNA-155 delivery, the effect of exogenous miRNA-155 overexpression on DCs is evaluated.

Main methods: For this purpose, exogenous miRNA-155 was electroporated with various voltages (0.100, 0.200, and 0.300 kV) into tumor cell-derived exosomes with various concentrations, and then DCs were treated with miRNA-155 loaded exosomes. To assess the effect of miRNA-155 loaded exosomes on DCs, the expression levels of IL12p70, IFN-γ, and IL10 in culture supernatants were measured by ELISA. Then, the expression profiles of DC surface markers, including CD11C, MHCII (I/A-I/E), CD86, CD40, and CD83 were investigated by flow cytometry.

Key findings: Concerning the results, exogenous miRNA-155 can be successfully inserted into tumor cell derived exosomes. Loading conditions for tumor cell-derived exosomes were enhanced for utilization as vehicles to deliver miRNA-155 into DCs. Analysis of the surface molecule revealed that miRNA-155 can increase the expression levels of MHCII (I/A-I/E), CD86, CD40, and CD83. ELISA analysis indicates that miRNA-155 can significantly increase, the levels of IL12p70, IFN-γ, and IL10.

Significance: Finally, it can be stated that miRNA-155 could be a candidate for dendritic cell maturation. This method can be applied in the modification of target cells in *in vitro* studies.

1. Introduction

Dendritic cells (DCs) are specialized antigen-presenting cells, which present antigens to natural killer (NK) cells, B-cells and T-cells. Therefore, DCs is considered as an outstanding candidate cells for immunotherapy of cancers [1]. However, the clinical efficiency of DC vaccination therapy needs to be improved, especially, with regards to the types of antigens which are used to prime DCs and the utilization of macromolecules such as microRNAs (miRNAs) for better activation and maturation of DCs [2–5].

Exosomes are nano-sized homogenous membrane vesicles (30–120 nm) derived from the exocytosis of intraluminal vesicles (within multi-vesicular bodies), then attached to the plasma membrane to be released into the extracellular space. Many cell types produce

* Correspondence to: S.M. Hashemi, Department of Immunology, School of Medicine, Shahid Beheshti University of Medical Sciences, Department of Applied Cell Sciences, School of Advanced Technologies in Medicine, Shahid Beheshti University of Medical Sciences, Tehran, Iran.
** Correspondence to: D. Amani, Department of Immunology, School of Medicine, Shahid Beheshti University of Medical Sciences, Tehran, Iran.
E-mail addresses: smmhashemi@sbmu.ac.ir (S.M. Hashemi), amanid@sbmu.ac.ir (D. Amani).

https://doi.org/10.1016/j.lfs.2019.01.005
Received 23 October 2018; Received in revised form 14 December 2018; Accepted 5 January 2019
Available online 06 January 2019

exosomes through this mechanism [6–8]. Since the exosome innately transport RNA molecules among cells and body fluids, it has been hypothesized that this feature might be suitable for gene delivery. Thus, exosomes have been previously used to transfer miRNA and other oligonucleotides to the target cells [9,10]. In comparison with other gene transport methods including lipid nanoparticles, viruses and polymeric nanoparticles, several advantages have been demonstrated for exosomes gene delivery system. Exosomes are not subject to attack by complement, opsonins, coagulation factors and antibodies in the body fluids [8,11–13]. There are different strategies which are used for loading antigen to dendritic cells including exosomes, viral vector-delivered whole antigen, tumor lysate, whole antigen–protein and using DNA or RNA [15,22,26,27]. Tumor cell-derived exosomes have a broad antigen repertoire for priming DCs in which they can expand both $CD8^+$ and $CD4^+$ T cells against cancer cells. Apart from the mentioned advantages of gene delivery, tumor cell-derived exosome contains several DC's maturation factors including HSP and GM-CSF, that can mature DC effectively [3,22,26–28].

miRNAs are a group of small noncoding RNAs, 20–25 nucleotide-long, and has key regulatory roles in different cell processes including cell survival, proliferation, apoptosis, tumor growth and metastasis [17]. In recent years, research to improve RNA-based therapy has been meaningfully increased [9,14,21,26,27]. It is noteworthy that, the main problem is an immune stimulation against the synthetic delivery vehicle and synthetic miRNAs, particularly if needed to repeat the dosing several times to treat disease [18]. Natural carriers can overcome these obstacles during miRNA delivery to cells. Exosomes as a natural RNA carrier might provide an available source of effective delivery plans [9].

So far, many miRNA studies on DCs have focused on the miRNA-155. miRNA-155 could modulate the IL-1 signaling pathway in stimulated human DCs [19]. miR-155 could enhance IL-12p70 and NF-κB production in DCs [20]. But the role of miR-155 in antigen presentation by DCs and DC maturation remains controversial [19,21,22].

To the best of the authors' knowledge, there is no experiment on delivering the miRNA-155 by tumor cells derived exosome into dendritic cells.

Here, delivery of miRNA-155 to DCs with exosomes, for simultaneous miRNA-155 delivery and antigen priming of DCs was optimized. Following treatment with miRNA-155 mimic loaded cancer derived exosomes, DCs were evaluated functionally and phenotypically.

2. Materials and methods

2.1. Cell culture and exosome isolation

CT26 cell line was obtained from Pasteur Institute (Tehran, Iran). Then, cells were cultured in Roswell Park Memorial Institute 1640 (RPMI 1640) (Gibco, NY, USA) complemented with 100 U/ml penicillin (Gibco®, NY, USA), 10% fetal bovine serum (Gibco®, NY, USA) and 100 mg/ml streptomycin (Gibco, NY, USA) then incubated at 37 °C in 5% CO_2. CT26 cells were adapted to the serum-free medium during a two-week period. Adapted cells line were grown to 70% confluences, and then incubated for 72 h in serum-free media. CT26 condition media were collected for exosome isolation according to the manufacturer's guidelines of exosome isolation kit (Exospin, Cell Guidance Systems LLC, MO, USA).

2.2. Dynamic light scattering of exosomes

Isolated exosomes size was identified by dynamic light scattering (DLS) Zetasizer Nano ZS (Malvern Instruments, UK). Before measuring the size of exosome by Zetasizer, protein concentration of the exosome content solution was diluted to 1 μg/ml. The distribution of exosome size was analyzed at 23 °C according to the manufacturer's instructions [23]. Experiments were carried out in triplicate.

2.3. Scanning electron microscopy (SEM) of exosomes

Shape and size of the isolated and electroporated exosomes were identified by scanning electron microscopy (SEM) (KYKY-EM 3200); the exosomes solution, 1 μg per ml, was left to dry on a glass slide for 24 h, then analyzed by SEM after covering the surface with a thin layer of gold. Experiments were carried out in triplicate.

The protein content of purified exosomes was evaluated with Bicinchoninic Acid (BCA) Protein Assay Kit (Sigma-Aldrich, Missouri, USA).

2.4. Atomic force microscopy of exosomes

The structure of exosomes was estimated by atomic force microscopy. In this method, exosomes were re-diluted with de-ionized water then left to dry on mica sheets. After fixing with 0.5% glutaraldehyde, they were washed with de-ionized water and left at room temperature (RT) to dry. The samples were scanned with a semi-contact strategy by scanning microscope (Solver Bio series, NT-MDT, Russia).

2.5. Optimization of the loading exosomes with miRNA-155

For exosomes loading with miRNA-155 mimic (Exiqon, Vedbaek, Denmark) to gain successful outcome, the miRNA loading condition for CT26 cell line derived exosomes was elaborated.

Exosome was re-suspended in 1:1 ratio with hypoosmolar Electroporation buffer (Eppendorf, Hum burg, Germany). Final concentration of miRNA-155 (100 pmol) was added to two distinctive concentrations of exosome (0.5 and 1 μg/ml). The mixtures were then moved into cold electroporation cuvettes (0.2 cm) and electroporated at different voltages (0.100–0.300 kV). An Eppendorf AG 22331 electroporation instrument (Eppendorf, Hum burg, Germany) was utilized for electroporation.

To eliminate free-floating miRNA-155 mimic outside the exosomes, the exosomes were treated with one unit of RNase H and re-isolated using Exospin™ kit. The relative amount of encapsulated miRNA-155 with SNORD housekeeping miRNA was determined by Stem-Loop Real-Time polymerase chain reaction (PCR) assays. To check that, the exosomes structure was not changed after electroporation; the shape and size of electroporated exosomes were identified by scanning electron microscopy.

2.6. Bone marrow-derived DCs (BMDCs) induction

Female BALB/c mice, 6–8 weeks of age, were purchased from The Pasture Institute, Tehran, Iran. The animals were stored at 22 ± 1 °C and relative humidity of 60 ± 5% under a 12 h light/dark cycle. Water and food were provided *ad libitum*. Animal experiments were carried out after approval from the Institutional Animal Ethics Committee.

BMDCs were prepared according to the method of Lutz et al. [24]. Bone marrow cells were obtained from female BALB/c mice and cultured in six-well Petri dishes in RPMI1640 with 10% FBS, supplemented with recombinant mouse GM-CSF (25 ng/ml) (PeproTech, NJ, USA) and IL-4 (25 ng/ml) (PeproTech, NJ, USA). After 7 days, 0.1 μg/ml LPS (Sigma-Aldrich, Missouri, USA) was added to induce DCs maturation. Shape and size of DCs were evaluated with phase contrast microscopy. To evaluate the Surface marker of DCs by flow cytometry, cells were stained with CD11c-APC (Bio Legend, CA, USA), MHCII (I-A/I-E)-PE (Bio Legend, CA, USA), CD86-FITC (Bio Legend, CA, USA), CD40-FITC (Bio Legend, CA, USA), CD83-PE (Bio Legend, CA, USA) and Fc blocking reagents (Bio Legend, San Diego, CA, USA). To prime DCs with exosomes, DCs were treated overnight with 100 μg/ml exosomes [25].

2.7. Exosome uptake by DC

To evaluate transfer of exosome into DCs, exosome was labeled with

PKH67 dye (Sigma-Aldrich, Missouri, USA) based on the manufacturer's protocol, and then DCs were treated with labeled exosomes. PKH-positive cells were detected after 24 h by fluorescence microscopy. In addition to determining the nucleus, DC's nucleus was labeled with a 4′,6-diamidino-2-phenylindole (DAPI) dye (Sigma-Aldrich, Missouri, USA) [26].

2.8. Tracking FAM-labeled miRNA in DCs

To evaluate the delivering of miRNA into DCs, FAM-labeled miRNA-155 was purchased (Exiqon, Vedbaek, Denmark). FAM-labeled miRNA was electroporated into exosomes, and then DCs were treated with FAM-labeled miRNA loaded exosomes. After 24 h, FAM-labeled miRNA was tracked into DCs by fluorescence microscopy.

2.9. Evaluation of miRNA-155 in DCs with real-time PCR

After treatment of the DCs with electroporated exosomes for 24 h, cells were washed twice with ice-cold phosphate-buffered saline (PBS) and miRNA was isolated with the miRNA isolation kit (miRNeasy Mini Kit, Qiagen, MD, USA) then cDNA was produced with the cDNA synthesis kit (Thermo Fisher Scientific, CA, USA). Quantitative real-time PCR using SYBR Green (Takara Bio, Japan) was performed in a 0.2 ml tube and run in a Corbett Rotor Gene 6000 (Celtic Molecular Diagnostics, Cape Town, South Africa) at 95 °C for 30 s, followed by 40 cycles of 95 °C for 5 s and 60 °C for 30 s. Each experiment was done in duplicate. According to the ΔΔCt method, the level of miRNA expression was measured utilizing the threshold cycle (Ct) [27]. SNORD was used as a housekeeping miRNA control, to normalize the relative expression of miRNAs.

2.10. Evaluation of DCs surface marker

To assess the effect of miRNA-155 loaded exosome on DCs, immature DCs were treated with tumor cell-derived exosome (exo) loaded with miRNA-155 mimic (mir) for 48 h. Flow cytometry evaluation of DCs surface marker, including CD11C, CD40, CD83, CD86 and MHCII (I/A-I/E) was done in the following groups: immature DCs (iDC), immature DCs treated with 100 μg/ml tumor cell-derived exosome (iDC/exo), immature DCs treated with 100 μg/ml tumor cell-derived exosome loaded with miRNA-155 mimic (iDC/exo/mir) and mature DCs (mDC) which treated for 48 h with 0.1 μg/ml LPS. Cells were labeled with the antibodies for 30 min at 4 °C; then, washed with washing buffer twice and detected by flow cytometry (BD, CA, USA). The data were analyzed by the FlowJo software Version 7.2.2.

2.11. Cytokine evaluation

Levels of mouse IL12p70, IFN-γ, and IL10 in DCs culture supernatants were measured using an enzyme-linked immunosorbent assay (ELISA) kit based on the manufacturer's instructions (Bio Legend, CA, USA).

2.12. Lymphocyte proliferation test

In order to monitor the ability of DCs in different groups to activate lymphocytes, the lymphocyte proliferation test was used. For lymphocyte proliferation test, lymphocytes from the spleen of female C57BL/6 mice were labeled with carboxyfluorescein diacetate succinimidyl ester (CFSE) (Thermo Fisher Scientific, CA, USA). For CFSE labeling, lymphocytes were re-suspended to 20×10^6/ml in 20 °C RPMI 1640 medium enriched with 10% FBS. A final concentration of 5 μM of dye was added to 1 ml aliquots of lymphocytes, then, mixed rapidly to ensure homogeneous labeling of cells. Cells were incubated at RT for 10 min, then washed 3 times with RPMI 1640 supplemented with 5% FBS. Labeling process has been described previously in details [28]. For lymphocyte proliferation test, DCs from different groups including iDC, iDC/exo, iDC/exo/mir and mDCs, treated with Mitomycin-C (Kyova, Tokyo, Japan), then co-cultured with CFSE-labeled responder lymphocytes in 1:10 ratio. The mixed cultures were incubated for 48 h in a 96-well plate at 37 °C and 5% CO_2. After cell staining with CD3-percp (Bio Legend, CA, USA) and gaiting the T lymphocyte, the proliferation of T lymphocyte was evaluated with CFSE dilution by flow cytometry.

2.13. Software and statistical analysis

All the data were expressed as the mean ± standard deviation (SD). After a logarithmic transformation to normalize the data, based on the data distribution, one-way analyses of variance (ANOVA) test was performed to make comparisons between groups. Two groups were compared by Student's *t*-test (Graph Pad Prism 4.0, CA, USA). p values < 0.05 were considered significant.

3. Results

3.1. CT26 cell-derived exosomes characterization

The average size of exosomes was 47 nm, as measured by dynamic light scattering (DLS), which was in the range of exosome size (Fig. 1A).

The spherical shape and size of isolated and electroporated exosomes (< 100 nm) were identified by scanning electron microscopy (Fig. 1B–C). The CT26 cell lines exosome was examined by atomic force microscopy and the size range (< 100 nm) and circular shape in 2-dimensional structure were confirmed (Fig. 1D).

3.2. Optimization of miRNA-155 mimic loading on CT26 cell-derived exosomes

To optimize the miRNA loading procedure, tumor cell-derived exosomes were electroporated with miRNA-155 mimics (100 pmol) at three different voltages (0.100, 0.200, and 0.300 kV). After electroporation, 1 mM EDTA was added to the electroporation cuvette to prevent interaction of aluminum ions with miRNA and buffer component [29]. Quantification of packed miRNA-155 into the exosomes was performed by quantitative Real-Time PCR assay. Among the three different applied voltages and two different exosomes concentration, 0.200 kV with 1 μg/ml of exosome was shown to be more significantly effective as compared to the others ($p < 0.05$) (Fig. 2).

3.3. Morphology and phenotypic characterization of DC

Phase contrast microscopy was used to characterize the morphology of DCs. In the differentiation process of DC, gradually, the cytoplasmic veils appeared on the surface of DCs. It showed that on day 7, DCs were larger cells and some cells displayed dendrites formation (Fig. 3). In addition, DCs surface markers were detected by flow cytometry. Analysis of the surface molecule reveals that iDC has low expression of MHC class II, CD86, CD83 and CD40 (Fig. 4). The mDC displayed a higher expression of the MHC class II, CD80 and CD40 when compared with the immature DC (Fig. 4).

3.4. Exosomes uptake by DC

To visualize the cellular uptake of exosomes, they were labeled with a green fluorescent lipid dye (PKH67). DCs were treated with PKH-labeled exosomes, and became fluorescent after 24 h (Fig. 5A, B, and C). Cells fluorescent intensity was associated with a higher level of PKH-labeled exosomes uptake (Fig. 5D, E, and F). These data indicate that exosomes were internalized by DCs. For more details, DC nucleus was labeled with DAPI dye (Fig. 5G).

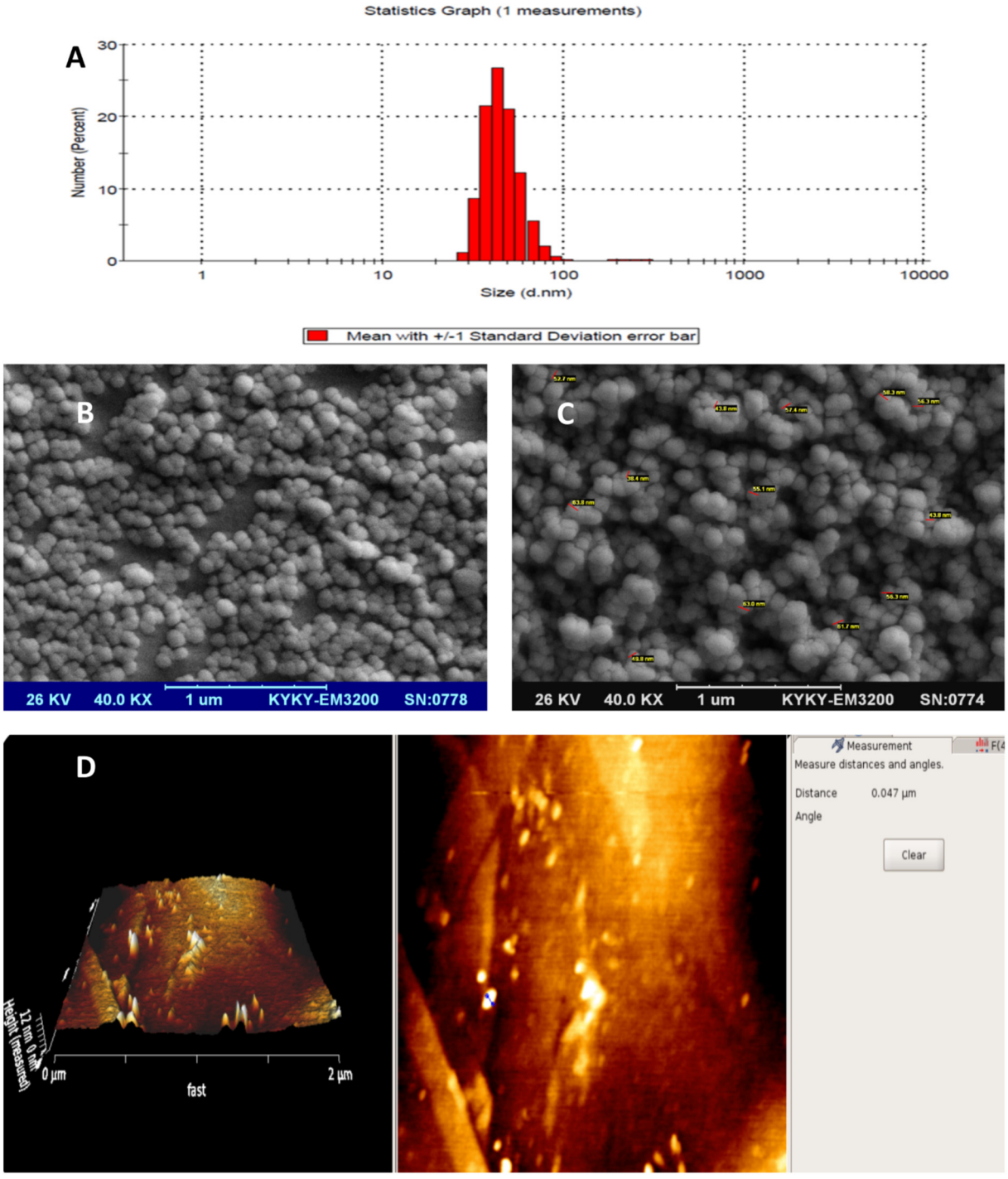

Fig. 1. Characterization of CT26 cell line exosomes. (A) The average size of exosomes was measured by DLS. (B&C) The spherical shape and size of isolated (B) and electroporated (C) exosomes were identified by scanning electron microscopy. Exosome was examined by atomic force microscopy and the size range and circular shape in 2-dimensional structure were confirmed (D).

3.5. Tracking of FAM-labeled miRNA in DCs

For visualization, miRNA delivery into DCs FAM-labeled miRNA-155 was tracked in DCs by fluorescence microscopy (Fig. 6). The findings indicated that FAM-labeled miRNA-155 was internalized by exosome into DCs.

3.6. Increased miRNA-155 expression levels in DCs

Following the treatment of DCs with exosomes, the expression level of miRNA-155 was determined by quantitative real time PCR assay. After 24 h of treatment, RNA was extracted and reverse transcribed to cDNA by specific miRNA-155 stem loop RT-PCR. As shown in Fig. 7, the miRNA-155 expression level significantly increased in exosome-treated cells relative to the controls ($p < 0.001$), indicating an efficient uptake of exosomes by DCs.

3.7. Morphology of DCs in different groups

Phase contrast microscopy was used to characterize the morphology

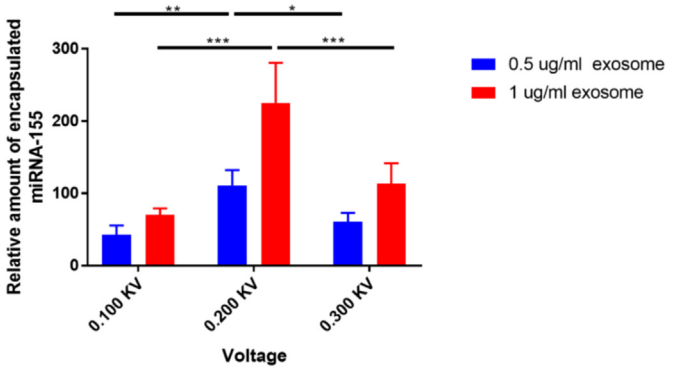

Fig. 2. The mean ± SD value of relative amount of encapsulated miRNA-155 in exosomes. Exosomes in two distinctive concentrations (0.5 and 1 μg/ml) were electroporated with miRNA-155 mimics (100 pmol) at three different voltages (0.100, 0.200, and 0.300 kV). After electroporation, the exosomes were re-isolated using Exospin™. Quantification of packed miRNA-155 into the exosomes was performed by quantitative Real-Time PCR assay. Among the three different applied voltages and two different exosomes concentration, 0.200 kV with 1 μg/ml of exosome was shown to be more significantly effective as compared to the others. The experiments were repeated four times in duplicate manner (*$p < 0.05$, ** $p < 0.01$, *** $p < 0.001$).

of DCs. Microscopic finding indicates that the cytoplasmic veils appeared on the surface of DCs in the iDC group and some cells displayed dendrite formation. Decrease in veils and increase fine surface dendritic processes were detected in the iDC/exo group. Fine surface dendritic processes with macropinosomes and vacuolated cytoplasm indicate maturation Process in the iDC/exo/mir group. In Addition, in the mDC group macropinosomes and many vacuoles in cytoplasm indicate maturation Process. Analysis of the morphology reveals that miRNA-155 can induce mature DCs as well as LPS (Fig. 3).

3.8. Analysis of DC surface marker in different groups

Analysis of DC surface markers including CD11C, CD83, CD40, CD86, and MHCII (I/A-I/E) in the iDC, iDC/exo, iDC/exo/mir, and mDC groups was conducted. Finding yielded by flow cytometric analysis of MHCII (I/A-I/E) levels in the iDC/exo/mir group indicates that the of MHCII (I/A-I/E) level increased significantly ($p < 0.001$) as compared to the iDC and iDC/exo groups, while the difference between the MHCII (I/A-I/E) level in the iDC/exo/mir group and the mDC group was not statistically significant. Flow cytometric analysis of the CD86 molecule levels in the iDC/exo/mir group revealed that it increased significantly ($p < 0.001$) when compared with the iDC and iDC/exo groups, while its increase relative to the mDC group was not statistically significant. Similarly, according to the flow cytometry analysis findings pertaining to the CD40 and CD83 molecule levels in the iDC/exo/mir group, the level of these surface molecules increased significantly ($p < 0.001$) when compared with the iDC and iDC/exo groups, but not relative to the mDC group. Finally, the flow cytometry analysis of iDC/exo and iDC group reveals that the exosome can significantly increase the CD40 and CD86 levels. Analysis of the surface molecule reveals that miRNA-155 can induce mature DCs as well as LPS. The flow cytometry data presented above indicate that, in the studied groups, DCs loaded with the miRNA-155 mimic exhibit uniformity in terms of size and density when compared with the other groups (Fig. 4).

3.9. Analysis of cytokine assays

Cell culture supernatants from different groups (iDC, iDC/exo, iDC/exo/mir, and mDC) were collected after 72 h and the levels of mouse IL12p70, IFN-γ, and IL10 were analyzed. The analysis of IL12p70 level in the iDC/exo/mir group indicates that it increased significantly ($p < 0.001$) when compared with the iDC and iDC/exo groups. The ELISA analysis of IL12p70 level in the mDC group similarly reveals that it increased significantly ($p < 0.001$) as compared to the other groups. IFN-γ level in the iDC/exo group increased significantly ($p < 0.001$) relative to the iDC group. Similarly, The ELISA analysis of IFN-γ level in the iDC/exo/mir group also reveals that it increased significantly ($p < 0.001$) when compared with the iDC and iDC/exo groups. Moreover, IFN-γ level in the mDC group increased significantly ($p < 0.001$) as compared with the other groups, whereas IL10 level in the iDC/exo group increased significantly ($p < 0.001$) relative to the iDC group. Finding yielded by ELISA analysis of IL10 level in the iDC/exo/mir group indicates that it increased significantly ($p < 0.001$) when compared with the iDC and iDC/exo groups, and the IL10 level in the mDC group increased significantly ($p < 0.001$) when compared with the other groups. In sum, based on the findings reported above, according to the ELISA analysis of iDC/exo and iDC groups, the exosome can significantly increase the IFN-γ and IL10 levels, while revealing that, in the iDC/exo/mir and iDC/exo groups, miRNA-155 can significantly increase the IL12p70, IFN-γ, and IL10 levels, as shown in Fig. 8.

3.10. Analysis of the T lymphocyte proliferation test results

Lymphocyte proliferation test was applied to monitor the ability of DCs to activate T lymphocytes. For the lymphocyte proliferation test, DCs from different groups including iDC, iDC/exo, iDC/exo/mir, and

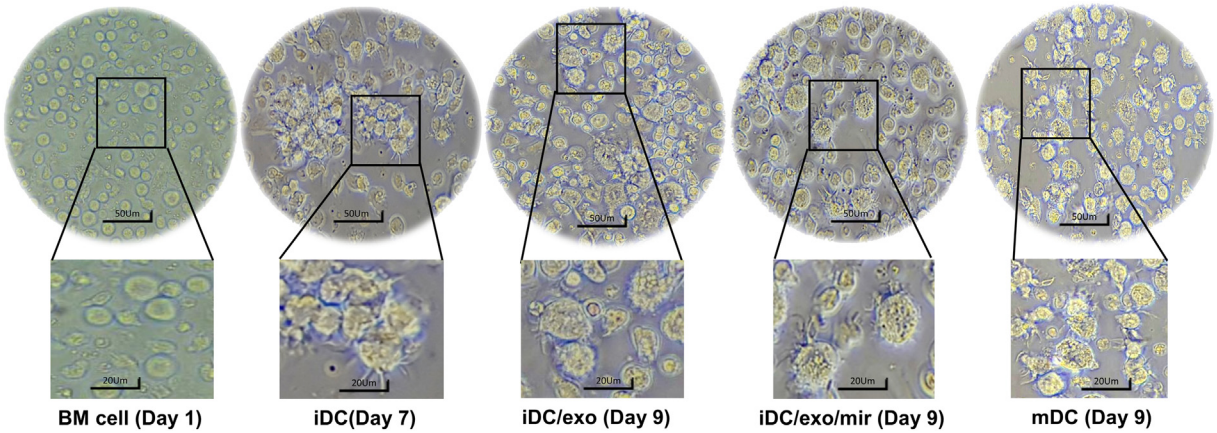

Fig. 3. Morphology of DCs in different groups. Phase contrast microscopy was used to characterize the morphology of DCs in different groups including: Bone marrow cells (BM cell), immature DCs (iDC), immature DCs treated with 100 μg/ml tumor cell-derived exosomes (iDC/exo), immature DCs treated with 100 μg/ml tumor cell-derived exosomes were loaded with miRNA-155 mimic (iDC/exo/mir) and mature DCs (mDC) which were treated 48 h with 0.1 μg/ml LPS.

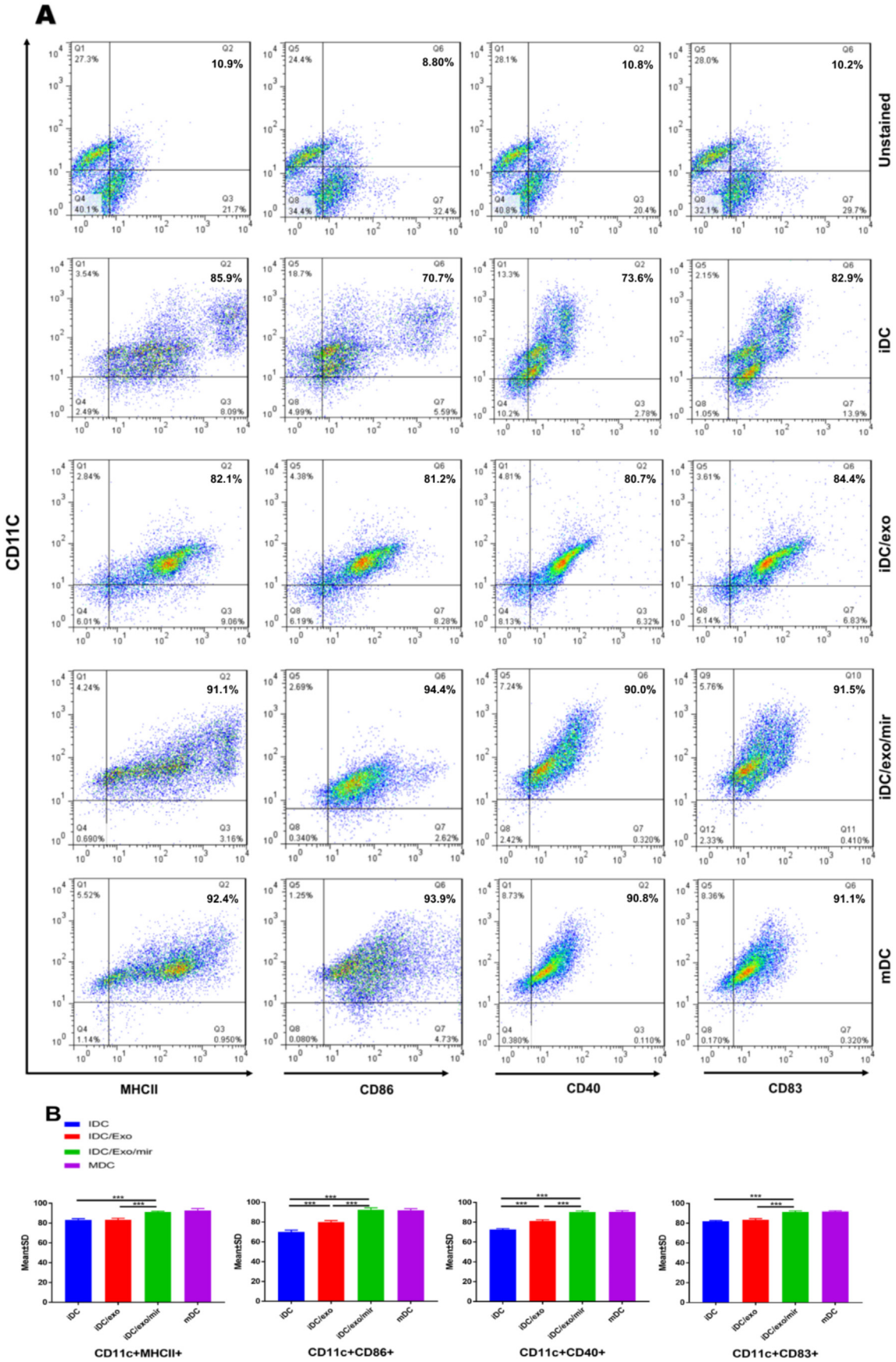

Fig. 4. Dot plot diagrams (A) and the mean ± SD triplicate value (B) of DCs surface marker of DCs in different groups. Analysis of surface markers (CD11C, MHCII (I/A-I/E), CD86, CD40 and, CD83) in different groups including: immature DCs (iDC), immature DCs treated with 100 μg/ml tumor cell-derived exosomes (iDC/exo), immature DCs treated with 100 μg/ml tumor cell-derived exosomes were loaded with miRNA-155 mimic (iDC/exo/mir) and mature DCs (mDC), which were treated 48 h with 0.1 μg/ml LPS, was done by flow cytometry (*** $p < 0.001$).

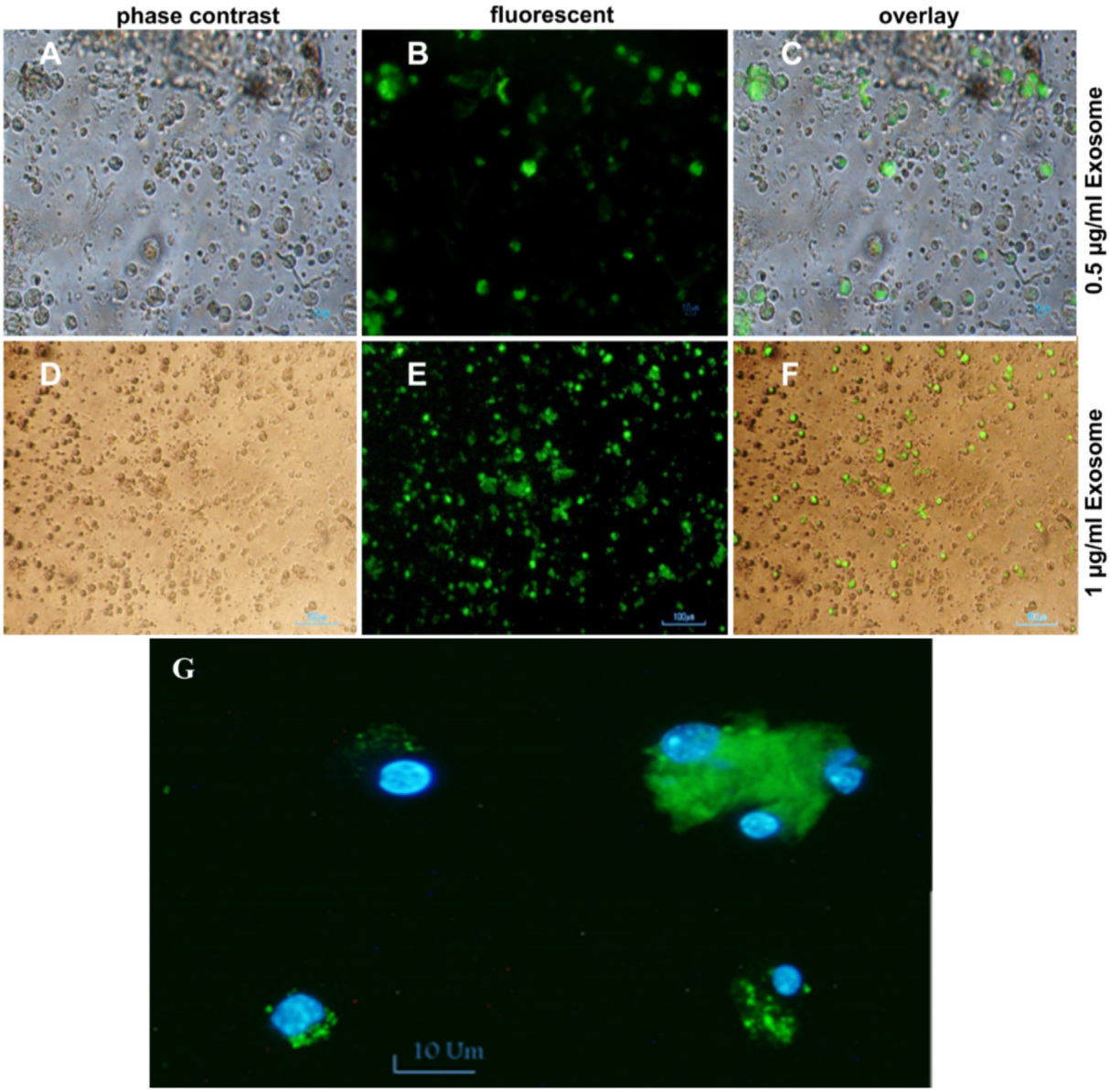

Fig. 5. PKH labeling of exosome and uptake exosomes by DCs. Exosomes were labeled with a green fluorescent lipid dye (PKH67). DCs were treated with PKH-labeled exosomes (0.5 µg/ml), and became fluorescent after 24 h. (A: phase contrast microscopy/B: fluorescent microscopy/C: overlay of A and B). Cells fluorescent intensity was associated with a higher level of PKH-labeled exosomes (1 µg/ml) uptake (D: phase contrast microscopy/E: fluorescent microscopy/F: overlay of D and E). DC nucleus was labeled with DAPI dye (G).

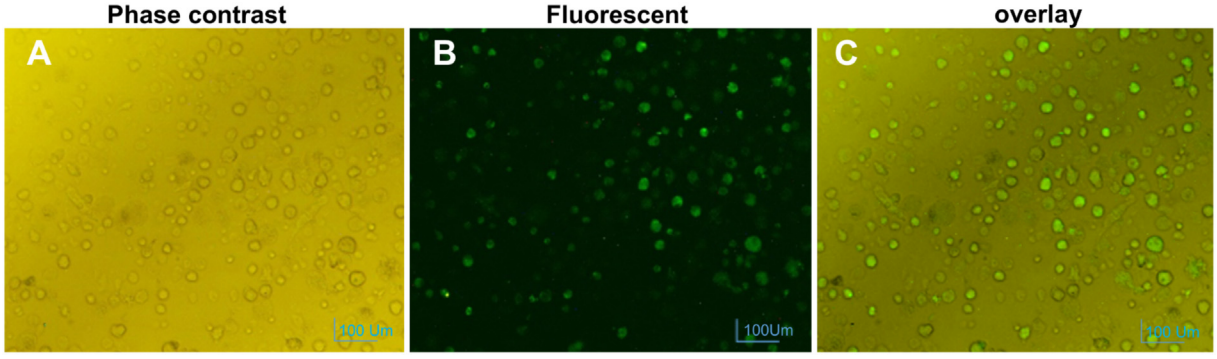

Fig. 6. Tracking FAM-labeled miRNA into DCs. FAM-labeled miRNA-155 was tracked in DCs by fluorescence microscopy. FAM-labeled miRNA was electroporated into exosomes, and then DCs were treated with FAM-labeled miRNA loaded exosomes. After 24 h, FAM-labeled miRNA was tracked into DCs by fluorescence microscopy. A: phase contrast microscopy B: fluorescent microscopy (green color indicates FAM-labeled miRNA). C: overlay of A and B. (For interpretation of the references to color in this figure legend, the reader is referred to the web version of this article.)

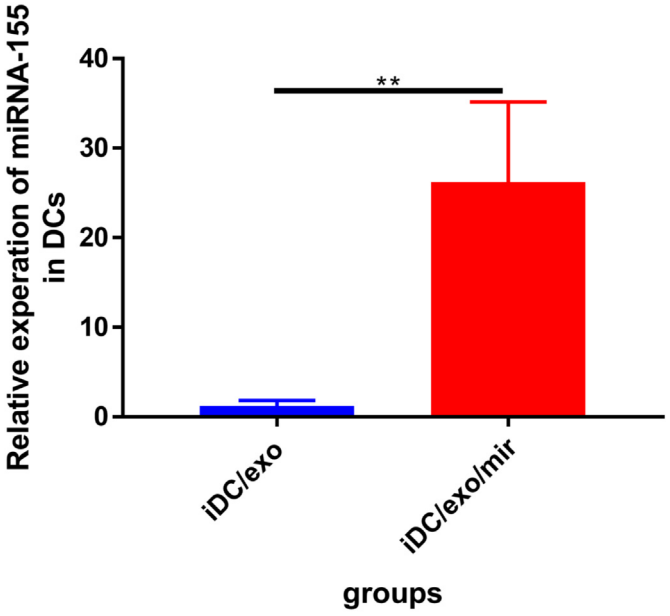

Fig. 7. The mean ± SD value of relative expression of miRNA-155 into DCs. After treatment of the DCs with electroporated exosomes for 24 h, cells were washed twice with ice-cold phosphate-buffered saline (PBS) and miRNA was isolated with the miRNA isolation kit, then cDNA was produced with the cDNA synthesis kit. Quantitative real-time PCR using SYBR Green was performed in a 0.2 ml tube. Analysis of data showed that electroporated exosomes could significantly increase the relative expression of miRNA-155 into DCs compared with the control group. The experiments were repeated four times in duplicate manner (*** $p < 0.001$).

mDCs were co-cultured with CFSE-labeled responder lymphocytes in a 1:10 ratio. Finding yielded by flow cytometry analysis of proliferation data revealed that the ability to proliferate T lymphocytes in the iDC/exo/mir group increased significantly ($p < 0.001$) relative to the iDC and iDC/exo groups. Moreover, the results showed that the ability to proliferate T lymphocytes in the iDC/exo group increased significantly ($p < 0.001$) as compared to the iDC group. Flow cytometry analysis of proliferation data revealed that the ability to proliferate T lymphocytes in iDC/exo/mir group decreased significantly ($p < 0.05$) as compared to the mDC group. However, no significant differences in the ability to proliferate T lymphocytes between the positive control and mDC groups were noted. Thus, according to the proliferation data analysis, in comparison with the mDCs, DCs loaded with the miRNA-155 mimic are less able to proliferate T lymphocytes (Fig. 9).

4. Discussion

The purpose of this study was to optimize delivering of the miRNA-155 mimic by tumor cells derived exosome into DCs *in vitro* and evaluate the effect of overexpression of miRNA-155 mimic on DCs.

miRNA-155 could enhance IL-12p70 and NF-κB production in DCs. Considering the noticeable miRNA-155 role's in the signaling pathways of DCs, miRNA-155 mimic was chosen in this study as the exogenous bio-macromolecules [24,29,38].

In previous studies, it was indicated that exosomes can naturally transfer a diversity of bio-molecules such as proteins, genomic DNA, mitochondrial DNA, mRNA and miRNA, [29–33].

However, exosome-mediated transfer efficacy has not been determined systemically, which can be different from the exosome source and the recipient cell type [34]. Exosome based macromolecule delivery has several benefits as compared to other delivery methods. First, exosome has non-toxicity when compared with other transfection reagent. Second, because exosome has a natural membrane, it can easily be pass through the plasma membrane and cause efficient RNA transport. Third, exosome can be separated from cell culture or the body fluids of each recipient, then used for loading the biological drug [17–20,22,23,26,28]. Also, tumor exosomes have a broad antigen repertoire for priming dendritic cells, they have HSP, GM-CSF and IL6 for better loading of antigens and the maturation of DCs [3,22,26–28]. Thus, simultaneous miRNA delivery and antigen priming of dendritic cells with tumor exosome is very affordable and useful.

In this study, the electroporation conditions were optimized in terms of electroporation voltage and exosome concentration for miRNA loading into exosomes. Using the optimum condition led to the highest amount of miRNA-155 transportation into the exosomes. To ensure this amount of miRNA is certainly the fraction of miRNA that is encapsulated inside the exosomes, suspension of exosomes after loading was treated with RNase H to distract free miRNA-155 [36]. Also, EDTA we added to the electroporation buffer to avoid precipitation of miRNA-155 during the electroporation procedure [29].

The results proved that exogenous miRNA-155 could be successfully inserted into tumor cells derived exosomes. According to the results of this study, 0.200 kV with 1 μg/ml of exosome is the best ratio to obtain the most effective miRNA transfected rate ($p < 0.001$). Results on

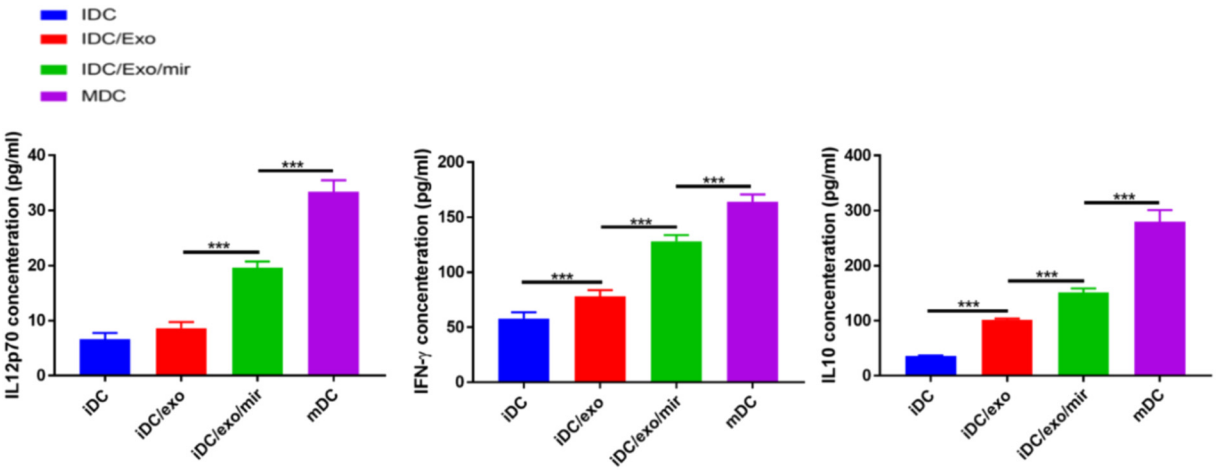

Fig. 8. The mean ± SD triplicate value of cytokines level by ELISA. Levels of mouse IL12p70, IFN-γ, and IL10 in cell culture supernatants after 72 h from different groups including: immature DCs (iDC), immature DCs treated with 100 μg/ml tumor cell-derived exosomes (iDC/exo), immature DCs treated with 100 μg/ml tumor cell-derived exosomes loaded with miRNA-155 mimic (iDC/exo/mir) and mature DCs (mDC) were measured using an enzyme-linked immunosorbent assay (ELISA) kit (*** $p < 0.001$).

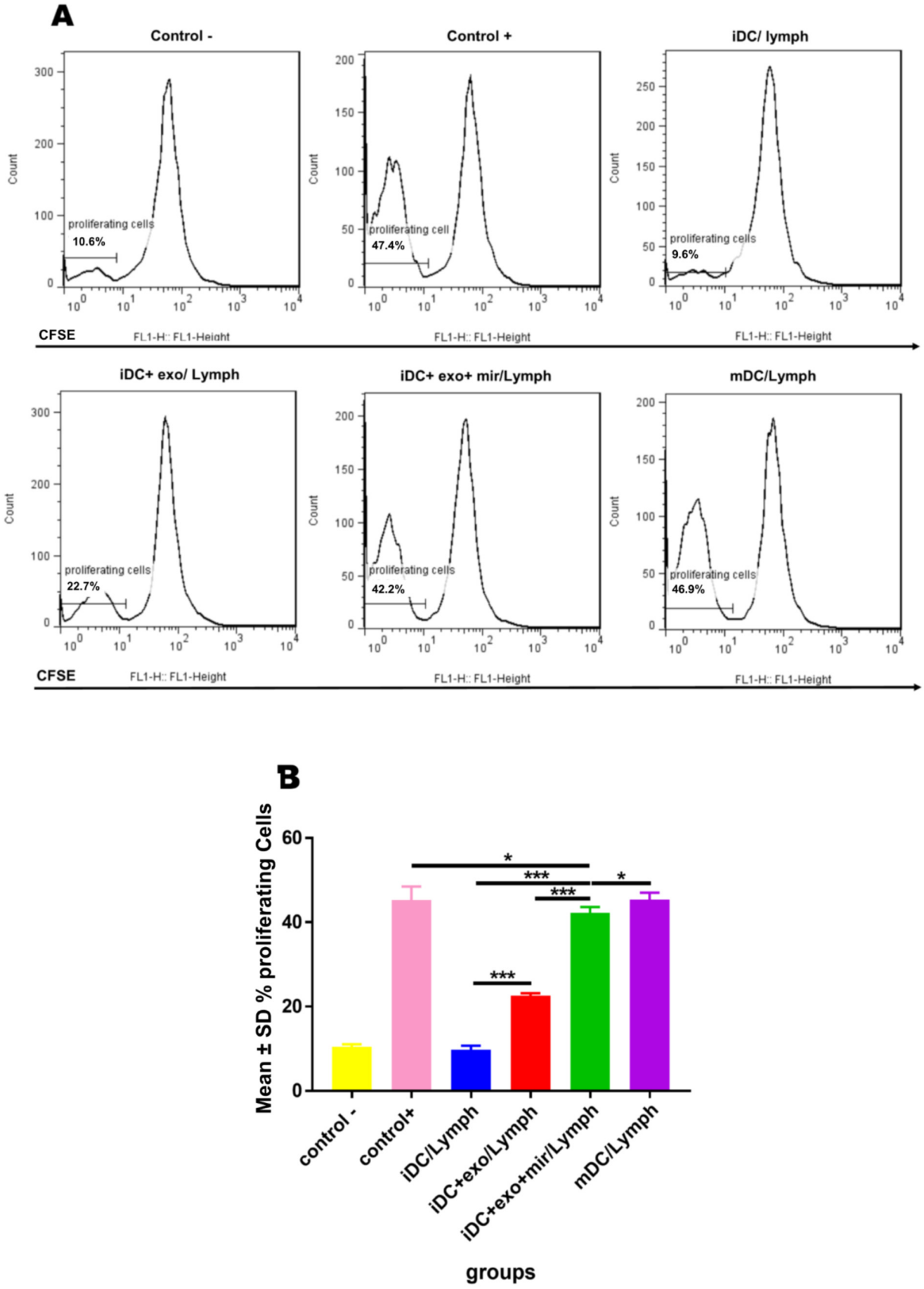

Fig. 9. Histogram (A) and, the mean ± SD triplicate value (B) of the T lymphocyte proliferation test. DCs from different groups including: immature DCs (iDC), immature DCs treated with 100 μg/ml tumor cell-derived exosomes (iDC/exo), immature DCs treated with 100 μg/ml tumor cell-derived exosomes loaded with miRNA-155 mimic (iDC/exo/mir) and mature DCs (mDC), treated with Mitomycin-C, then co-cultured with CFSE-labeled responder lymphocytes in 1:10 ratio. After cells staining with CD3-percp and gaiting the T lymphocyte, the proliferation of T lymphocyte was evaluated with CFSE dilution by flow cytometry. Control negative: CFSE-labeled responder lymphocytes without any treatment. Control positive: CFSE-labeled responder lymphocytes treated with 2% PHA (Gibco®, NY, USA). Lymph: Lymphocyte (*$p < 0.05$, *** $p < 0.001$).

electroporation voltage and exosome concentration support those of other studies which are similar in delivering method, but different in the type of miRNA, exosome and cell line [32,33,35,37].

This study demonstrated that tumor cell-derived exosomes could function as vehicles to deliver exogenous miRNA-155 into DCs. The efficacy of exosome in miRNA delivery was confirmed by treatment of DCs with miRNA-155 loaded exosomes. The level of miRNA-155 increased > 100-fold in the DCs after treatment with miRNA-155 loaded exosome.

A potent maturation stimulus for DCs is LPS with 0.1 μg/ml concentration [16,29,38]. LPS induced maturation was assessed by examining MHCII (I/A-I/E), CD40, CD83, and CD86 expression. So, the maturation effect of miRNA-155 was compared with LPS. It is reported that the level of MHCII (I/A-I/E), CD86, CD40, and CD83 in DCs treatment with miRNA-155 loaded exosomes increased significantly ($p < 0.001$) in comparison with DCs treatment with exosomes alone. These results provide more evidence for Dueck's study, which showed that miRNA155-dependent miRNA hierarchy could mature DCs [29] and Sauthier's study, which showed that miRNA-155 is critical for dendritic cell maturation [38]. Our results revealed that the levels of MHCII (I/A-I/E), CD86, CD40, and CD83 in DCs treated with miRNA-155 mimic loaded exosomes were not significant ($p > 0.05$) as compared to mature DCs treated with LPS. CD83 is the major surface marker for identifying mature DCs [39]. In this study, it is reported that the miRNA-155 mimic can increase the level of CD83 in DCs significantly ($p < 0.001$). The results shown that the miRNA-155 mimic can induce DCs maturation as well as LPS which has been also observed in previous studies [20,38].

Mature DCs could increase allogeneic lymphocyte stimulation and produce IL12, that could be a T lymphocyte stimulating factor and has effect on the differentiation of T helper 0 cells into T helper 1 cells [39,41]. To evaluate the effect of miRNA-155 on cytokine production by DCs, the level of mouse IL12p70, IFN-γ, and IL10 was evaluated using ELISA. The result showed that miRNA-155 mimic could increase the expression of IL-12p70 and IFN-γ by DCs. This result indicates that DCs treated with miRNA-155, could fortify the proliferation of T lymphocyte and start T helper 1 reactions. These results are compatible with previous studies [3,24,43]. The result showed that the level of IL10 increased in treated groups.

Next, the ability of DCs in different groups to activate and proliferate lymphocytes was examined. Our result reveals that the ability of proliferation T lymphocyte in DCs treated with miRNA-155 loaded exosomes increased significantly ($p < 0.001$) when compared with DCs treated with exosomes. Analysis of proliferation data indicates that DCs treated with miRNA-155 mimic loaded exosomes can proliferate T lymphocyte significantly when compared with immature DCs. This result showed that the miRNA-155 mimic can induce immunogenic DCs, which can activate and proliferate lymphocyte. The results support those of Rodriguez et al. [21]. The result showed that miRNA-155 mimic could increase the expression of IL-12p70 and IFN-γ by DCs. These DCs are more capable of activating and proliferating lymphocyte and have effects on the differentiation of naive T cells into T helper 1 cells [40].

These results offer compelling proof that, the miRNA-155 was successfully loaded into tumor exosome, and then, loaded exosome can transfer miRNA-155 into DCs *in vitro*.

5. Conclusion

In conclusion, the present study optimized the loading status for tumor exosomes, and employed them as transporter to transport miRNA-155 into DCs. It is shown that the DCs with overexpression of miRNA-155 mimic in term of phenotype and function is similar to mDCs. In addition, the miRNA-155 mimic can induce immunogenic DCs, which can activate and proliferate lymphocyte as well as LPS. Finally, it can be stated that miRNA-155 could be a candidate for dendritic cell maturation.

Acknowledgments

The present research is financially supported by “Research Department of the School of Medicine, Shahid Beheshti University of Medical Sciences” (Grant No. 8993) and “National Institute for Medical Research Development” (Grant No. 962574).

Appendix A. Supplementary data

Supplementary data to this article can be found online at https://doi.org/10.1016/j.lfs.2019.01.005.

References

[1] N. Rains, R.J. Cannan, W. Chen, R.S. Stubbs, Development of a dendritic cell (DC)-based vaccine for patients with advanced colorectal cancer, Hepato-Gastroenterology 48 (2001) 347–351.
[2] D. Gao, C. Li, X. Xie, P. Zhao, X. Wei, W. Sun, H.-C. Liu, A.T. Alexandrou, J. Jones, R. Zhao, J.J. Li, Autologous tumor lysate-pulsed dendritic cell immunotherapy with cytokine-induced killer cells improves survival in gastric and colorectal cancer patients, PLoS One 9 (2014) e93886, , https://doi.org/10.1371/journal.pone.0093886.
[3] X. Gu, U. Erb, Improved Vaccine Efficacy of Tumor Exosome Compared to Tumor Lysate Loaded Dendritic Cells in Mice, 84 (2015), pp. 74–84, https://doi.org/10.1002/ijc.29100.
[4] M. Tewari, S. Sahai, R.R. Mishra, S.K. Shukla, H.S. Shukla, Dendritic cell therapy in advanced gastric cancer: a promising new hope? Surg. Oncol. 21 (2012) 164–171, https://doi.org/10.1016/j.suronc.2012.03.003.
[5] K. Palucka, J. Banchereau, Cancer immunotherapy via dendritic cells, Nat. Rev. Cancer 12 (2012) 265–277, https://doi.org/10.1038/nrc3258.
[6] S. Nojehdehi, S. Soudi, A. Hesampour, S. Rasouli, M. Soleimani, S.M. Hashemi, Immunomodulatory effects of mesenchymal stem cell–derived exosomes on experimental type-1 autoimmune diabetes, J. Cell. Biochem. 119 (11) (2018) 9433–9443.
[7] C. Théry, S. Amigorena, G. Raposo, A. Clayton, Isolation and characterization of exosomes from cell culture supernatants and biological fluids, Curr. Protoc. Cell Biol. (2006) 3–22.
[8] A.-K. Ludwig, B. Giebel, Exosomes: small vesicles participating in intercellular communication, Int. J. Biochem. Cell Biol. 44 (2012) 11–15, https://doi.org/10.1016/j.biocel.2011.10.005.
[9] L. Jiang, P. Vader, R.M. Schiffelers, Extracellular vesicles for nucleic acid delivery: progress and prospects for safe RNA-based gene therapy, Gene Ther. 24 (2017) 157–166.
[10] F. Shahabipour, N. Barati, T.P. Johnston, G. Derosa, P. Maffioli, A. Sahebkar, Exosomes: nanoparticulate tools for RNA interference and drug delivery, J. Cell. Physiol. 232 (7) (2017) 1660–1668.
[11] S. Kourembanas, Exosomes: vehicles of intercellular signaling, biomarkers, and vectors of cell therapy, Annu. Rev. Physiol. 77 (2015) 13–27, https://doi.org/10.1146/annurev-physiol-021014-071641.
[12] T.-H. Tran, G. Mattheolabakis, H. Aldawsari, M. Amiji, Exosomes as nanocarriers for immunotherapy of cancer and inflammatory diseases, Clin. Immunol. 160 (2015) 46–58, https://doi.org/10.1016/j.clim.2015.03.021.
[13] A.J. O'Loughlin, C.A. Woffindale, M.J.A. Wood, Exosomes and the emerging field of exosome-based gene therapy, Curr. Gene Ther. 12 (2012) 262–274.
[14] F. André, N. Chaput, N.E.C. Schartz, C. Flament, N. Aubert, J. Bernard, G. Raposo, B. Escudier, D. Hsu, T. Tursz, S. Amigorena, E. Angevin, L. Zitvogel, F. Andre, N. Chaput, N. Aubert, J. Bernard, Exosomes as potent cell-free peptide-based vaccine. I. Dendritic cell-derived exosomes transfer functional MHC class I/peptide complexes to dendritic, Cell (2016), https://doi.org/10.4049/jimmunol.172.4.2126.
[15] F. André, N.E.C. Schartz, N. Chaput, C. Flament, G. Raposo, S. Amigorena, E. Angevin, L. Zitvogel, Tumor-derived exosomes: a new source of tumor rejection antigens, Vaccine 20 (2002) 28–31, https://doi.org/10.1016/S0264-410X(02)00384-5.
[16] D.W. Greening, S.K. Gopal, R. Xu, R.J. Simpson, W. Chen, Exosomes and their roles in immune regulation and cancer, Semin. Cell Dev. Biol. 40 (2015) 72–81, https://doi.org/10.1016/j.semcdb.2015.02.009.
[17] Y. Chi, D. Zhou, MicroRNAs in colorectal carcinoma-from pathogenesis to therapy, J. Exp. Clin. Cancer Res. 35 (2016) 43.
[18] Y. Seow, M.J. Wood, Biological gene delivery vehicles: beyond viral vectors, Mol. Ther. 17 (2009) 767–777.
[19] M. Ceppi, P.M. Pereira, I. Dunand-Sauthier, E. Barras, W. Reith, M.A. Santos, P. Pierre, MicroRNA-155 modulates the interleukin-1 signaling pathway in activated human monocyte-derived dendritic cells, Proc. Natl. Acad. Sci. 106 (2009) 2735–2740.
[20] A. Dueck, A. Eichner, M. Sixt, G. Meister, A miR-155-dependent microRNA hierarchy in dendritic cell maturation and macrophage activation, FEBS Lett. 588 (2014) 632–640, https://doi.org/10.1016/j.febslet.2014.01.009.
[21] A. Rodriguez, E. Vigorito, S. Clare, M.V. Warren, P. Couttet, D.R. Soond, S. van

Dongen, R.J. Grocock, P.P. Das, E.A. Miska, Requirement of bic/microRNA-155 for normal immune function, Science 316 (2007) 608–611.
[22] C. Lu, X. Huang, X. Zhang, K. Roensch, Q. Cao, K.I. Nakayama, B.R. Blazar, miR-221 and miR-155 Regulate Human Dendritic Cell Development, Apoptosis, and IL-12 Production Through Targeting of p27 kip1, KPC1, and SOCS-1, 117 (2015), pp. 1–4, https://doi.org/10.1182/blood-2010-12-322503.The.
[23] F. Martínez-gutierrez, E.P. Thi, J.M. Silverman, C.C. De Oliveira, S.L. Svensson, A. Vanden Hoek, E.M. Sánchez, N.E. Reiner, E.C. Gaynor, E.L.G. Pryzdial, E.M. Conway, E. Orrantia, F. Ruiz, Y. Av-gay, H. Bach, Antibacterial activity, inflammatory response, coagulation and cytotoxicity effects of silver nanoparticles, Nanomedicine 8 (2012) 328–336, https://doi.org/10.1016/j.nano.2011.06.014.
[24] M.B. Lutz, N. Kukutsch, A.L.J. Ogilvie, S. Rößner, F. Koch, N. Romani, G. Schuler, An advanced culture method for generating large quantities of highly pure dendritic cells from mouse bone marrow, J. Immunol. Methods 223 (1999) 77–92.
[25] O. Ashiru, P. Boutet, L. Fernández-Messina, S. Agüera-González, J.N. Skepper, M. Valés-Gómez, H.T. Reyburn, Natural killer cell cytotoxicity is suppressed by exposure to the human NKG2D ligand MICA* 008 that is shed by tumor cells in exosomes, Cancer Res. 70 (2010) 481–489.
[26] D.M. Pegtel, K. Cosmopoulos, D.A. Thorley-Lawson, M.A.J. van Eijndhoven, E.S. Hopmans, J.L. Lindenberg, T.D. de Gruijl, T. Würdinger, J.M. Middeldorp, Functional delivery of viral miRNAs via exosomes, Proc. Natl. Acad. Sci. 107 (2010) 6328–6333.
[27] R.T. Martinez-Nunez, F. Louafi, P.S. Friedmann, T. Sanchez-Elsner, MicroRNA-155 modulates the pathogen binding ability of dendritic cells (DCs) by down-regulation of DC-specific intercellular adhesion molecule-3 grabbing non-integrin (DC-SIGN), J. Biol. Chem. 284 (2009) 16334–16342.
[28] B.J.C. Quah, C.R. Parish, The use of carboxyfluorescein diacetate succinimidyl ester (CFSE) to monitor lymphocyte proliferation, J. Vis. Exp. 2010 (44) (2010) 2259.
[29] S.A.A. Kooijmans, S. Stremersch, K. Braeckmans, S.C. de Smedt, A. Hendrix, M.J.A. Wood, R.M. Schiffelers, K. Raemdonck, P. Vader, Electroporation-induced siRNA precipitation obscures the efficiency of siRNA loading into extracellular vesicles, J. Control. Release 172 (2013) 229–238.
[30] M.L. Turner, F.M. Schnorfeil, T. Brocker, M.L. Turner, F.M. Schnorfeil, T. Brocker, MicroRNAs regulate dendritic cell differentiation and function, J. Immunol. 187 (2011) 3911–3917, https://doi.org/10.4049/jimmunol.1101137.
[31] R. Crescitelli, C. Lässer, T.G. Szabó, A. Kittel, M. Eldh, I. Dianzani, E.I. Buzás, J. Lötvall, Distinct RNA profiles in subpopulations of extracellular vesicles: apoptotic bodies, microvesicles and exosomes, J. Extracell. Vesicles 2 (2013) 20677.
[32] A. Montecalvo, A.T. Larregina, W.J. Shufesky, D.B. Stolz, M.L.G. Sullivan, J.M. Karlsson, C.J. Baty, G.A. Gibson, G. Erdos, Z. Wang, Mechanism of transfer of functional microRNAs between mouse dendritic cells via exosomes, Blood 119 (2012) 756–766.
[33] H. Valadi, K. Ekström, A. Bossios, M. Sjöstrand, J.J. Lee, J.O. Lötvall, Exosome-mediated transfer of mRNAs and microRNAs is a novel mechanism of genetic exchange between cells, Nat. Cell Biol. 9 (2007) 654.
[34] M.E. Marcus, J.N. Leonard, FedExosomes: engineering therapeutic biological nanoparticles that truly deliver, Pharmaceuticals 6 (2013) 659–680.
[35] G. Raposo, W. Stoorvogel, Extracellular vesicles: exosomes, microvesicles, and friends, J. Cell Biol. 200 (2013) 373–383.
[36] F. Momen-heravi, S. Bala, T. Bukong, G. Szabo, Exosome-mediated delivery of functionally active miRNA-155 inhibitor to macrophages, Nanomedicine 10 (2014) 1517–1527, https://doi.org/10.1016/j.nano.2014.03.014.
[37] F. Momen-Heravi, S. Bala, T. Bukong, G. Szabo, Exosome-mediated delivery of functionally active miRNA-155 inhibitor to macrophages, Nanomedicine 10 (2014) 1517–1527.
[38] I. Dunand-Sauthier, M.-L. Santiago-Raber, L. Capponi, C.E. Vejnar, O. Schaad, M. Irla, Q. Seguín-Estévez, P. Descombes, E.M. Zdobnov, H. Acha-Orbea, Silencing of c-Fos expression by microRNA-155 is critical for dendritic cell maturation and function, Blood 117 (17) (2011) 4490–4500.
[39] M. Lechmann, N. Shuman, A. Wakeham, T.W. Mak, The CD83 reporter mouse elucidates the activity of the CD83 promoter in B, T, and dendritic cell populations in vivo, Proc. Natl. Acad. Sci. 105 (33) (2008) 11887–11892.
[40] R.A. Seder, R. Gazzinelli, A. Sher, W.E. Paul, Interleukin 12 acts directly on CD4+ T cells to enhance priming for interferon gamma production and diminishes interleukin 4 inhibition of such priming, Proc. Natl. Acad. Sci. 90 (1993) 10188–10192.
[41] X. Li, X. He, B. Liu, L. Xu, C. Lu, H. Zhao, X. Niu, S. Chen, A. Lu, Maturation of murine bone marrow-derived dendritic cells induced by Radix Glycyrrhizae polysaccharide, Molecules 17 (2012) 6557–6568, https://doi.org/10.3390/molecules17066557.